KEK Preprint 2000-97
TUAT-HEP 2000-3
OULNS 00-02
DPNU-00-32
BELLE Preprint 2000-2
September 2000
H

Magnetic Field Mapping of the Belle Solenoid

N. TAN, M. AKATSU, A. BOZEK, K. FUJIMOTO, J. HABA, T. HARA, H. HIRANO, M HIROSE, T. HOJO. K. HOSHINA, K. INAMI, A. ISHIKAWA, Y. IWASAKI, K.K. JOO, N. KATAYAMA, Y. MAKIDA, T. MATSUMOTO, I. NAGAI, K. NAKAI, O. NITOH, Y. OHNISHI, T. OKABE, N. OKAZAKI, H. OZAKI, Y. SAKAI, A. SUGI, A. SUGIYAMA, S. SUITOH, J. SUZUKI, S. SUZUKI, F. TAKASAKI, J. TANAKA, M. TOMOTO, K. TRABELSI, U. UNO, H. YAMADA, H. YAMAOKA, Y. YAMAOKA, T. YOKOYAMA and K. YOSHIDA

High Energy Accelerator Research Organization

High Energy Accelerator Research Organization (KEK)

KEK Reports are available from:

Information Resources Division
High Energy Accelerator Research Organization (KEK)
1-1 Oho, Tsukuba-shi
Ibaraki-ken, 305-0801
JAPAN

Phone: +81-298-64-5137
Fax: +81-298-64-4604
E-mail: adm-jouhoushiryou1@ccgemail.kek.jp
Internet: http://www.kek.jp

Magnetic field mapping of the Belle solenoid

N. Tan[a] M. Akatsu[b] A. Bozek[c,2] K. Fujimoto[b] J. Haba[c,1] T. Hara[d] H. Hirano[e] M. Hirose[b] T. Hojo[d] K. Hoshina[e] K. Inami[b] A. Ishikawa[b] Y. Iwasaki[c] K.K. Joo[c,3] N. Katayama[c] Y. Makida[c] T. Matsumoto[b] I. Nagai[b] K. Nakai[a] O. Nitoh[e] Y. Ohnishi[c] T. Okabe[b] N. Okazaki[e] H. Ozaki[c] Y. Sakai[c] A. Sugi[b] A. Sugiyama[b] S. Suitoh[b] J. Suzuki[c] S. Suzuki[b] F. Takasaki[c] J. Tanaka[f] M. Tomoto[b] K. Trabelsi[d,4] S. Uno[c] H. Yamada[d] H. Yamaoka[c] Y. Yamaoka[c] T. Yokoyama[e] K. Yoshida[b]

[a] *Department of Physics, Faculty of Industrial Science and Technology, Science University of Tokyo, Noda, Chiba 278-8510 Japan*

[b] *Department of Physics, Nagoya University, Nagoya 464-8602, Japan*

[c] *High Energy Accelerator Research Organization (KEK), Tsukuba, Ibaraki 305-0801, Japan*

[d] *Department of Physics, Faculty of Science, Osaka University, Machikaneyama, Toyonaka, Osaka 560-0043, Japan*

[e] *Department of Applied Physics, Faculty of Technology, Tokyo University of Agriculture and Technology, Koganei, Tokyo 184-8588, Japan*

[f] *Department of Physics, Faculty of Science, University of Tokyo, Tokyo, 113-8654, Japan*

Abstract

The mapping of the magnetic field of the Belle detector's large superconducting solenoid is described. The mapping was done with the accelerator magnets located inside the Belle solenoid excited to their nominal field values. To cope with geometrical constraints, we developed a novel moving mechanism for the field probes that uses an ultrasonic motor located in the strong magnetic field.

Key words: Belle, KEKB, magnetic field mapping
PACS: 07.55.-w, 29.30.Aj, 14.40.Nd, 13.25.Hw

1 Introduction

The main purpose of the Belle detector is to make precision studies of B meson decays with a special emphasis on testing standard-model predictions concerning violations of CP symmetry [1]. The detector sits at the single interaction region (IR) of the KEKB e^+e^- collider [2] at the High Energy Accelerator Research Organization (KEK). KEKB is a double-ring collider where each beam has a separate ring with a different energy so as to make asymmetric energy collisions. A novel feature of KEKB is the 22 mrad crossing angle of the beams at the interaction point (IP). In order to achieve a luminosity as high as $10^{34}\mathrm{cm}^{-2}\mathrm{sec}^{-1}$, the beams are focused sharply onto the IP by a pair of vertically focusing superconducting quadrupole coils located on each side of the IP.

The Belle detector has a solenoidal field around IP to provide momentum measurements of charged particle secondaries from B meson decays. Charged particle tracking is provided by a cylindrical drift chamber (CDC) [3] and a silicon vertex detector (SVD) [4]. In order to compensate for deleterious effects of the Belle solenoidal field on the optical properties of the KEKB beams, a pair of superconducting compensating solenoids are installed on either side of IP inside the same cryostat as the quadrupole coils. The leakage field from the compensating solenoid coils results in rather severe distortions of the magnetic field in the Belle tracking region. It was, therefore, necessary to map the field over the entire tracking volume with all the relevant magnetic components excited in situ.

2 The Belle spectrometer magnet and the QCS system

The layout of the magnetic components at the KEKB IR is shown in Fig. 1. The Belle spectrometer is comprised of a superconducting solenoid coil of 1.8 m radius and 3.9 m length located inside of an iron flux return yoke [5]. The flux return consists of three parts: a barrel and two end yokes, as illustrated in Fig. 1. These are assembled from 47 mm thick iron slabs in a fifteen-layer structure, with interspersed resistive plate chambers for K_L and μ particle detection [6]. The design field strength at the solenoid center is 1.5 Tesla at

[1] E-mail: junji.haba@kek.jp
[2] Present address: Krakow Inst. of Nuclear Physics, ul. Kawiory 26a, PL-30-055 Krakow, Poland
[3] Present address: Department of Physics, University of Toronto, Toronto, Ontario Canada M5S 1A7
[4] Present address: Univ. of Hawaii, 2505 Correa Road, Honolulu, HI 96822, U.S.A.

the nominal operating current of 4200 Amperes. The major parameters of the Belle solenoid are listed in Table 1.

Two superconducting magnet complexes (QCS-R and QCS-L) [7] are inserted in holes along the axis of the end yokes. Each magnet complex has a solenoidal coil for compensation of the Belle solenoidal field, a quadrupole for focusing the beams onto the IP, and several correction coils all located in a single cryostat. The major parameters of the QCS system are tabulated in Table 2. Among the QCS coils, the compensating solenoid has the largest distorting effect on the Belle solenoid field. The quadrupoles introduce an azimuthal dependence to the field.

3 The field mapping device

The goal for the high momentum tracking performance of the Belle detector is $\sigma_{p_t}/p_t \simeq 0.2\%$ where p_t denotes a transverse momentum. This translates to a point-by-point precision of the field map of 30 Gauss. A calculation indicates that the field gradients inside the tracking volume are as large as 30 Gauss/mm. The position accuracy of the mapping should, therefore, be less than 1 mm.

As noted above, we have to make the field map with the QCS system in place and with the quadrupoles and the compensating solenoid excited to their nominal field values. The volume that is mapped is reasonably isolated from outside because of the very limited gap between the pole tips and the QCS cryostat, as seen in Fig. 2. The resulting lack of access makes it necessary to make the field mapping device that is fully contained inside the Belle magnet; conventional magnetic motors could not be used to drive the motion.

The mapping system logic uses a cylindrical coordinate system centered along the Belle solenoid axis with origin at the IP. Side and end views of the system as it looks installed inside the Belle magnet are shown in Fig. 2. Figure 3 provides a schematic illustration of the measuring system's moving mechanism. It consists of a cylindrical rotating cage and supporting frame that fixed to the inside of the Belle magnet. The cage can rotate in ϕ direction and is supported at each end plate on two sets of roller guides that are fixed to the frame. The r-mover can slide in z-direction along the z-rail, which is fixed to the cage.

For the ϕ rotation of the cage, we used a high-torque AC servo-motor [11] that was placed outside of the pole piece in a region where the magnetic field was less than 300 gauss. This motor drove a pulley via a $1.5m$ long shaft that rotated the cage via a timing belt.

The z- and r-drive mechanisms were placed inside the rotation cage where magnetic field was as strong as 1.5 Tesla, where a conventional magnetic motor would not work. Here we used an ultrasonic motor (USM) as a driver. The USM we used [8] has a relatively high torque and a pulse control capability. Every element used in the motor was non magnetic including the bearing. Its measured performance characteristics are listed in Table 3. The whole r-mover system, including one USM, was mounted on the z-rail. The z-motion was provided via a timing belt driven by a USM fixed to the end of the rail. Figure 4 shows the details of the r-mover and the placement of the field probes. Because of the non-magnetic nature of the USM, the system was relatively simple compared to a system with all drivers located outside and coupled to the probes via a complicated mechanical transmission system. The measured performance of the mapping system is summarized in Table 4. All of the motions were pulse-controlled and monitored with rotary encoders by a PC.

The field probe was a commercial product [9] that contains three orthogonally oriented Hall sensors to measure the r, z and ϕ field components. We used three probes (#1, #2 and #3) offset in the r-direction as indicated in Fig. 4. The probes covered the radial ranges of $0 < r < 450$ mm (#1), $175 < r < 625$ mm (#2) and $450 < r < 900$ mm (#3). The Hall currents were digitized, converted to field strength, and sent to the PC through a GPIB interface [9].

We installed an NMR probe [10] on one of the connecting rods of the rotating cage at $r = 700mm$ and $z = 470mm$, as indicated in Fig. 2. This provided an absolute calibration of field strength with a precision better than 1 Gauss. It was also used to monitor the stability of the magnet during the measurement.

4 Calibration and Measurement

4.1 Alignment of the system

The alignment of the system inside the Belle magnet was adjusted and checked using a telescope that was aligned on the axis of the Belle magnet. Changes in the position of a target mark on probe #1, which was positioned at the center of ϕ-rotation ($r = 0$), was monitored while the r-mover was moved along z and rotated in ϕ. After adjusting the global position of the system, the shifts observed with the telescope for any motion in z or ϕ direction were less than 0.32 mm.

4.2 Probe alignment

Since the three sensors in a single 3D probe were not always perfectly orthogonal to each other, there could be a significant residual field in a minor component from a major one. Each probe was aligned independently so as to zero-out the effect of B_z on both B_ϕ and B_r sensor, while minimizing the effects of B_r on the B_ϕ sensor. These adjustments were made with the magnetic field generated by either the Belle solenoid or the compensation solenoid in the QCS system. The former provided a relatively uniform field along z-axis in the central region while the latter generated a field with a significant B_r component. In either case, B_ϕ could be assumed to be very small.

After the adjustment, we checked the systematics in the field strength due to a misalignment by rotating the probe around the z-axis. It was found that changes in field value measurements due to the rotation were less than ± 15 Gauss for any component.

4.3 Calibration of Hall sensors

We used the NMR probe to calibrate the #3 probe, which could be positioned at the position where the NMR probe was normally located. Since the B_z component is dominant at the NMR position, only the B_z sensor was calibrated. This was done by changing the current applied to the Belle solenoid from 2000 to 4300 ampere. Figure 5 shows the ratio of the #3 Hall probe reading to that of the NMR as a function of the NMR reading. The non-linear dependence observed here was fit with a third-order polynomial that was used to correct the B_z sensor of the #3 probe. The magnitude of the non-linearity expected for the sensors of other components was small enough to be neglected in the present application. The other probes (#1 and #2) were also corrected in turn with respect to the corrected reading of the #3 probe by using measurements from the regions of overlapping radial coverage shown in Fig. 5.

4.4 Field mapping

For most of the measurements, the magnets were operated at their nominal currents as tabulated in Table 5. This corresponds to a field strength of 1.5 Tesla at the interaction point and a field integral along the beam axis that is almost zero because of the effects of the compensation solenoids. Measurements with other current configurations were also made (also summarized in the Table 5) to accomodate possible future changes in magnet operating field strengths. For the nominal settings, the field was measured at 1500 points with

a $5cm(z) \times 5cm(r)$ mesh in 32 different ϕ planes. Finer, 5000 point maps with a mesh of 0.5 to $2.5cm$ near the QCS cryostat were also taken for every 45° angle in ϕ. The motion was programmed to stay for $5sec$ at each mesh point before measurement. The average scan rate was $10sec$ per point including the movement of the probe.

A daily measurement on the reference plane with coarse sampling was used to monitor the stability of the system. Figure 6 shows the distribution of differences between two such measurements made before and after a short shutdown of the Belle solenoid. Even with the maximum change in the current of the solenoid, the reproducibility of the measured field was found to be at the ± 1 Gauss level.

5 Reconstruction of field map

Figure 7 is a contour plot of the field measured inside the tracking volume for nominal magnet settings. The field strength as a function of z position is plotted in Fig. 8 for several radii. It is evident that the field gradient due to the compensation solenoids is large and the precise field mapping reported here is needed for a track reconstruction at the level required for Belle. In the vicinity of the QCS-R, a quadrupole distortion due to the quadrupole coils can be seen in Fig. 9, where the field strength is plotted as a function of ϕ. The observed field distortion is fit to a function of the form $A_0 cos(\phi + \alpha)$, where α is an offset angle (2°) of the quadrupole coil in the QCS-R determined by the KEKB beam optics. The z dependence of the fitted amplitudes A_0 for each component are shown for several radii in Fig. 10.

In the region where the quadrupole field is negligible, we average the measured field over ϕ. To justify this, deviations of the measured field strengths from their average values at different ϕ angles are examined. Figure 11 shows the distribution of these deviations for the B_z, B_r and B_ϕ measurements. It is found that the deviations are less than ± 10 gauss, which is less than the precision required for the mapping. This is another demonstration of the stability or reproducibility of the field map measurements.

6 Conclusions

The field mapping inside the Belle tracking volume was mapped with the nearby accelerator magnets excited. Because of geometrical constraints, a mapping device that was fully contained inside the magnetic volume was used.

The r- and z-motions of the field probes in the strong magnetic field were accomplished with by ultra sonic motors, resulting in a rather simple moving mechanism.

A 100,000 point field map was made in a month. The map has been used to improve the momentum resolution of charged tracks. Figure 12 shows an example of the tracking performance; here the reconstructed mass peak of J/ψ particles from B meson decays are plotted. The fitted value of the peak mass is 3.089 GeV/c^2, while the established value is 3.0969 GeV/c^2[12], indicating that the error in the absolute calibration of the present measurement is of order 0.25%.

Acknowledgments

We wish to thank the KEK Belle cryogenic group headed by Prof. Y. Doi for their excellent operation of the Belle solenoid. We express our thanks to Mr. Y. Watanabe and his colleagues at Toko Esco Ltd. for their help in design and fabrication of the field mapping device. Thanks also go to Drs. K. Tsuchiya, N. Ohuchi and T. Ogitsu (KEKB, QCS group) for their cooperation toward a better understanding of the magnetic field of the QCS system.

References

[1] The Belle Collaboration, Belle Technical Design Report, KEK Report 95-1 (1995).
J. Haba, Nucl. Instr. and Methods, A368(1995)74.

[2] KEKB B-Factory Design Report, KEK Report 95-7 (1995).

[3] S.Uno, Nucl. Instr. and Methods, A379 (1996) 421.
H. Hirano *et al.*, KEK preprint 2000-2, accepted for publication in Nucl. Instr. and Methods, Section A.

[4] G. Alimonti *et al.*, KEK preprint 2000-34.

[5] Y. Makida *et al.*, Adv. Cryog. Eng. Vol. 43A (1998)221.
H. Mukai *et al.*, in Proc of 15th Int'l Conf. on Magnet Technology (MT-15) 1998, p1044.
Y. Makida *et al.*, Performance of a Superconducting Solenoid Magnet for Belle Detector in KEKB B-factory, IEEE Trans. of Applied Superconductivity, Vol. 9 in press.

[6] A. Abashian *et al.*, Nucl. Instr. and Methods, A449 (2000) 112.

[7] T. Ogitsu *et al.*, in Proc of the 6th European Accelerator Conference (EPAC98), 1988, p2038.
K. Tsuchiya, T. Ogitsu, N. Ohuchi, T. Ozaki and N. Toge, Superconducting Magnets for the Interaction Region of KEKB, IEEE Trans. of Applied Superconductivity, Vol. 9 in press.

[8] Fukoku Co. Ltd. Motor department, 1508-2 Ooazaakabori Kurakake,Oura-chou, Oura-Gun,Gunma,Japan #370-0614.
http://www.fukoku-rubber.co.jp/english/seihin/etc02.htm

[9] ZOA99-3202 probe with Model 9953 Gaussmeter made by F.W. Bell, A Division of Bell Technologies, 6120 Hanging Moss Road, Orlando, Florida USA.
http://www.fwbell.com/

[10] Echo Electronics Co. Ltd. Kashiwa-cho 4-8-41, Shiki, Saitama 353-0007.
http://echo-denshi.co.jp/

[11] RKS-32-3030s made by Harmonic Drive System Inc. Minami-ooi, Shinagawa, Tokyo 140-0013, Japan.
http://www.hds.co.jp/hds.htm

[12] Caso *et al.*, Review of Particle Physics, The European Physical Journal C, vol.3, 1998.

Table 1
Major parameters of the Belle solenoid.

Cryostat	inner radius	1,700 mm
	outer radius	2,000 mm
Coil	main radius @ 4.5° K	1,800 mm
	length @ 4.5° K	3,910 mm
Conductor	cross section	$3 \times 33\text{mm}^2$
	winding pitch	3.3 mm
Electrical	No. of turns	1175
	Inductance	5.2 H
	Nominal current	4,200 A
	Central field	1.5 Tesla

Table 2
Major parameters of the QCS system

		QCS-L	QCS-R	
Compensation solenoid	central field	4.53	5.80	Tesla
	current	487	603	A
	inner diameter	190	190	mm
	outer diameter	230	230	mm
	length	461	616	mm
	No. of turns	3749	4981	
Quadrupole	Field gradient	21.78	21.78	T/m
	Current	2963	2963	A
	Effective length	486.1	387.7	mm
	Inner radius	130	130	mm

Table 3
Specification of the ultrasonic motor (USM)

model	USR-60NKE
Rated torque	3.2 kgfcm
Rated speed	> 90 rpm
Output power	3 W
Holding torque	> 3.2 kgfcm
Unit weight	240 g
Dimension	$67 \times 67 \times 45\text{mm}^3$

Table 4
Performance of Field mapping device

direction	r	z	ϕ
Motion range	450 mm	2710 mm	360°
Reproducibility	$< \pm 0.1$ mm	$< \pm 0.1$ mm	$\pm 30'$
Straightness of motion	< 0.06 mm	< 0.05 mm	NA
Deviation from circular motion	NA	NA	< 0.2 mm

Table 5
Operation condition for Field mapping

Variations	Belle solenoid (A)	compensation solenoid R/L (A)	Quadrupole (A)
Nominal	4160	613/495	3000
COMP+	4160	640/550	3000
COMP-	4160	550/450	3000
Solenoid+	4180	613/495	3000
Solenoid-	4140	613/495	3000
Q+	4160	613/495	3300
Q-	4160	613/495	2700
solenoid alone	4160	0	0
-0.25T	3440	512/413	3000
solenoid alone	3440	0/0	0
-0.5T	2740	410/330	3000
solenoid alone	2740	0/0	0

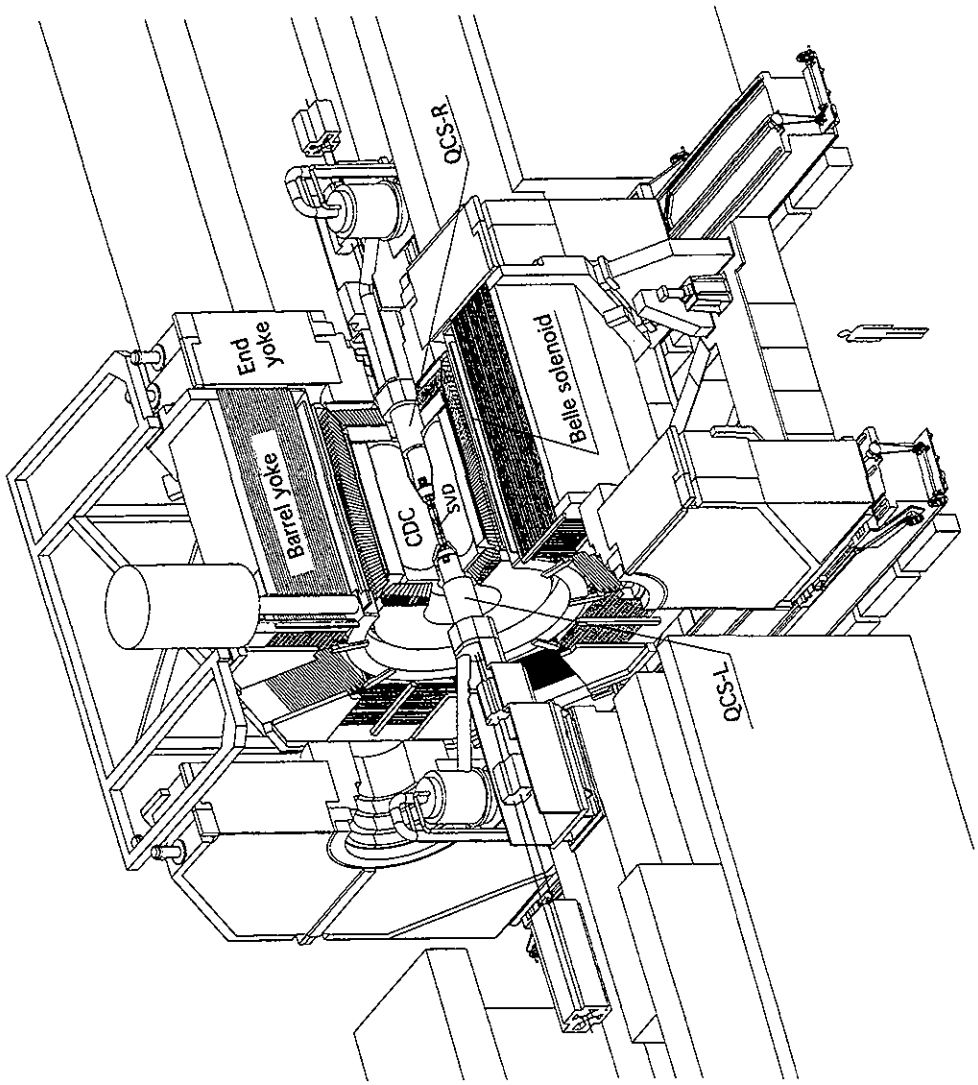

Fig. 1. The Belle detector and the interaction region of KEKB.

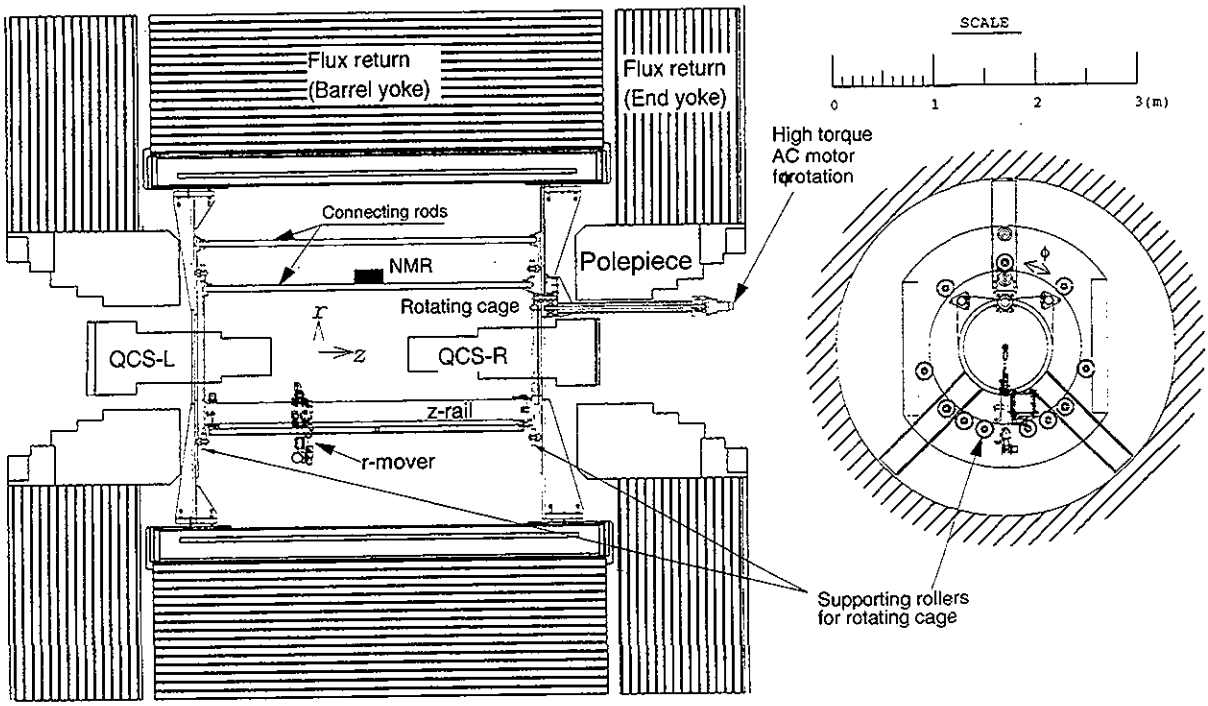

Fig. 2. Side and end views of the field mapping device. Some of the rods connecting both end plates are not shown.

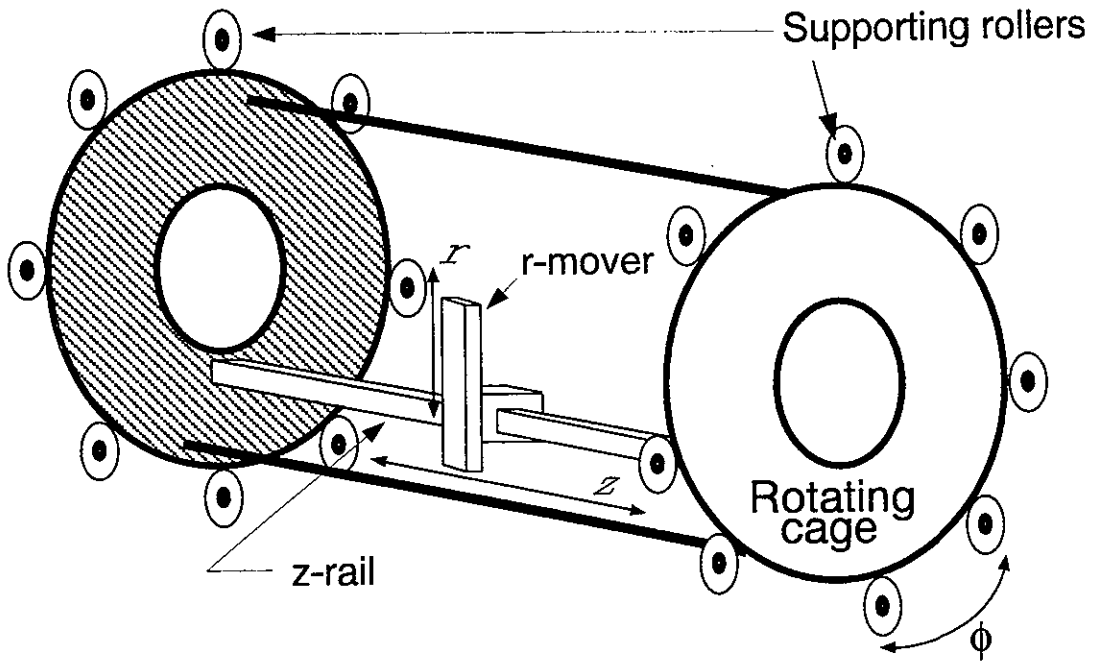

Fig. 3. A conceptual illustration of the field mapping device.

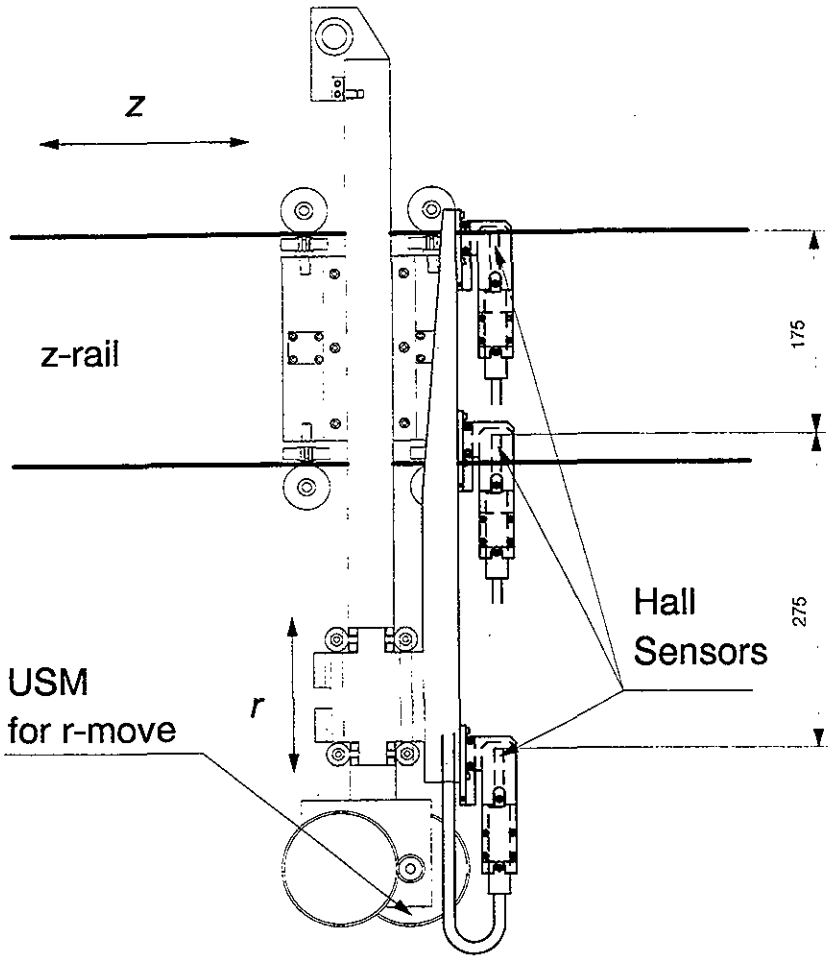

Fig. 4. A detailed drawing of the r-mover.

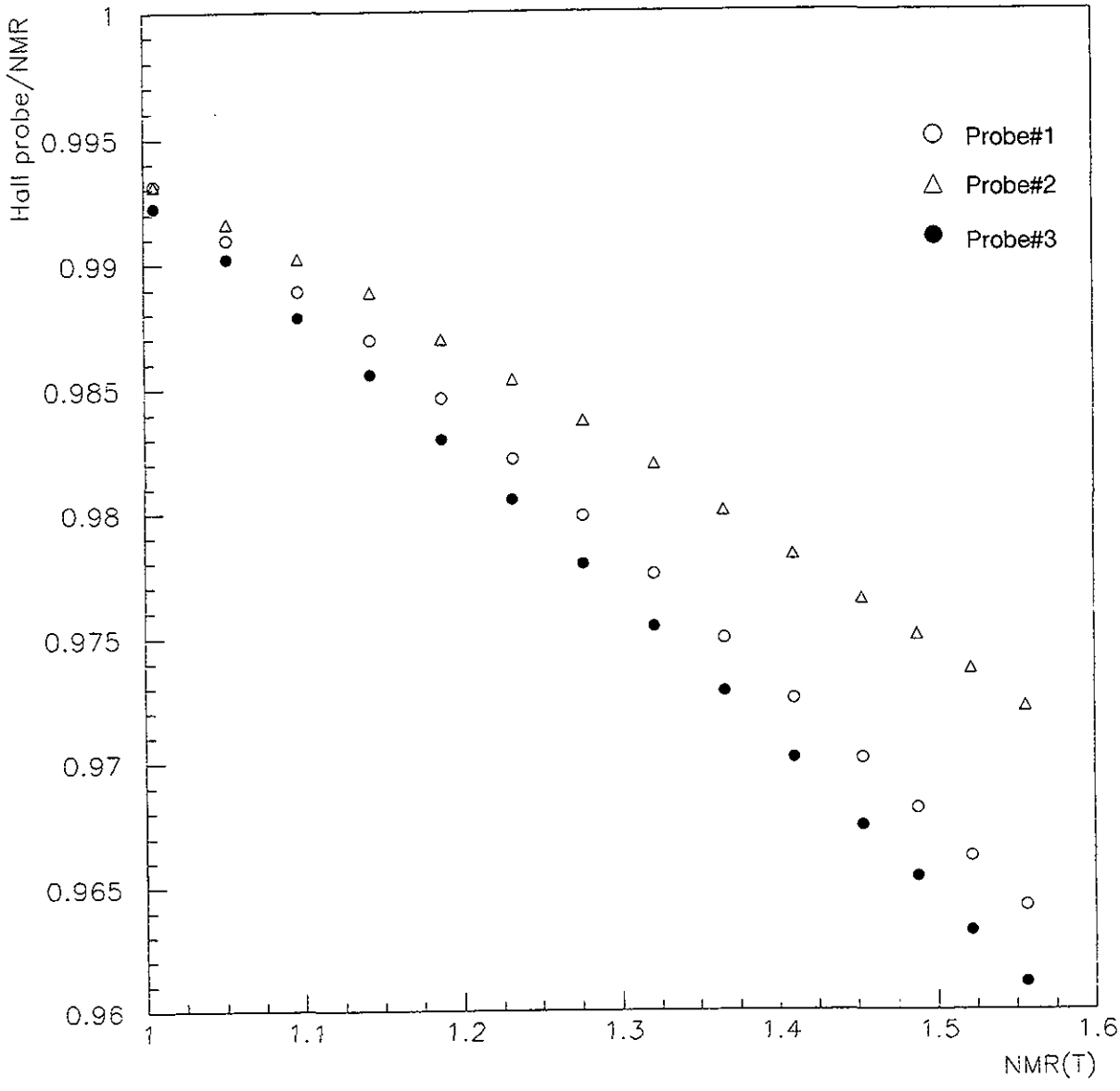

Fig. 5. The ratios of the Hall probe readings to that of the NMR as a function of the NMR reading.

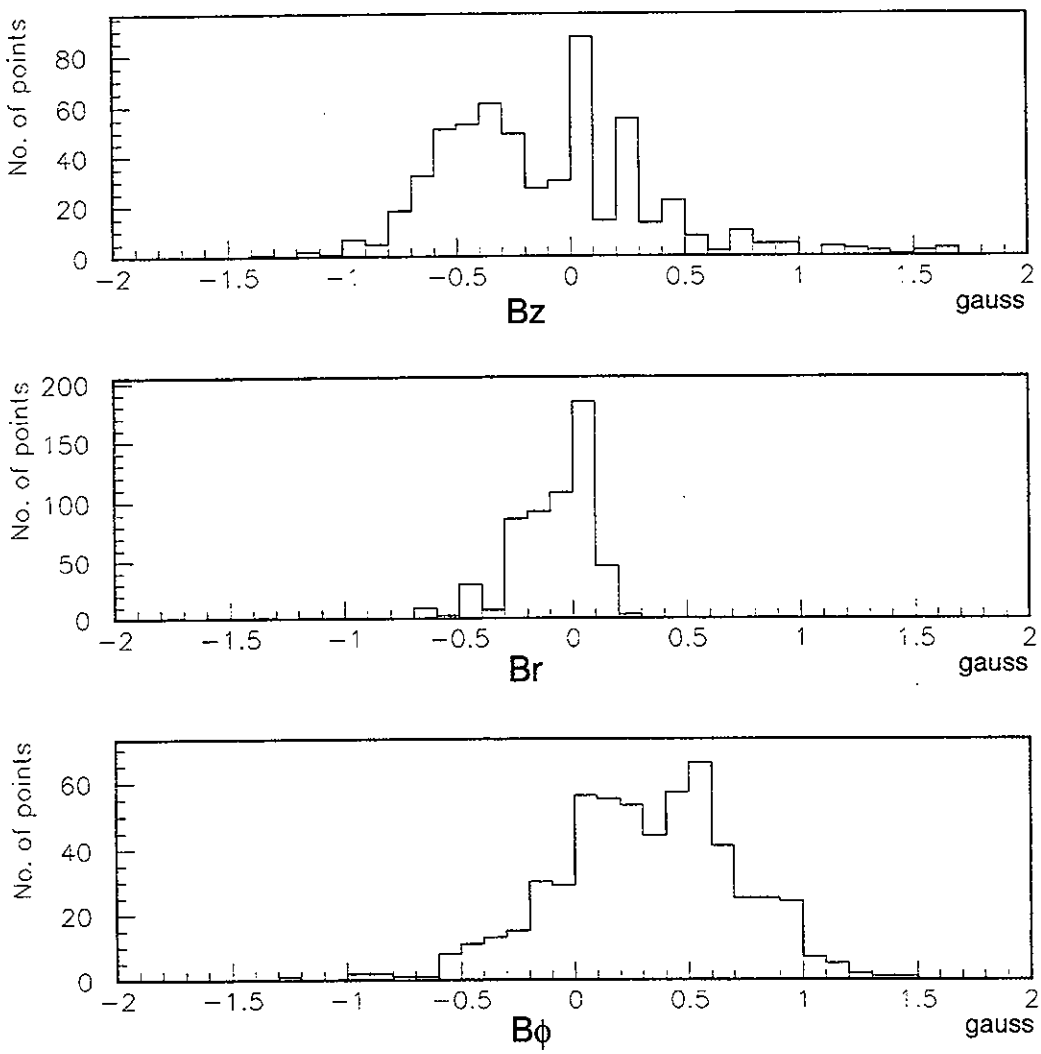

Fig. 6. Differences between measurements made before and afetr the shut-down of the Belle solenoid.

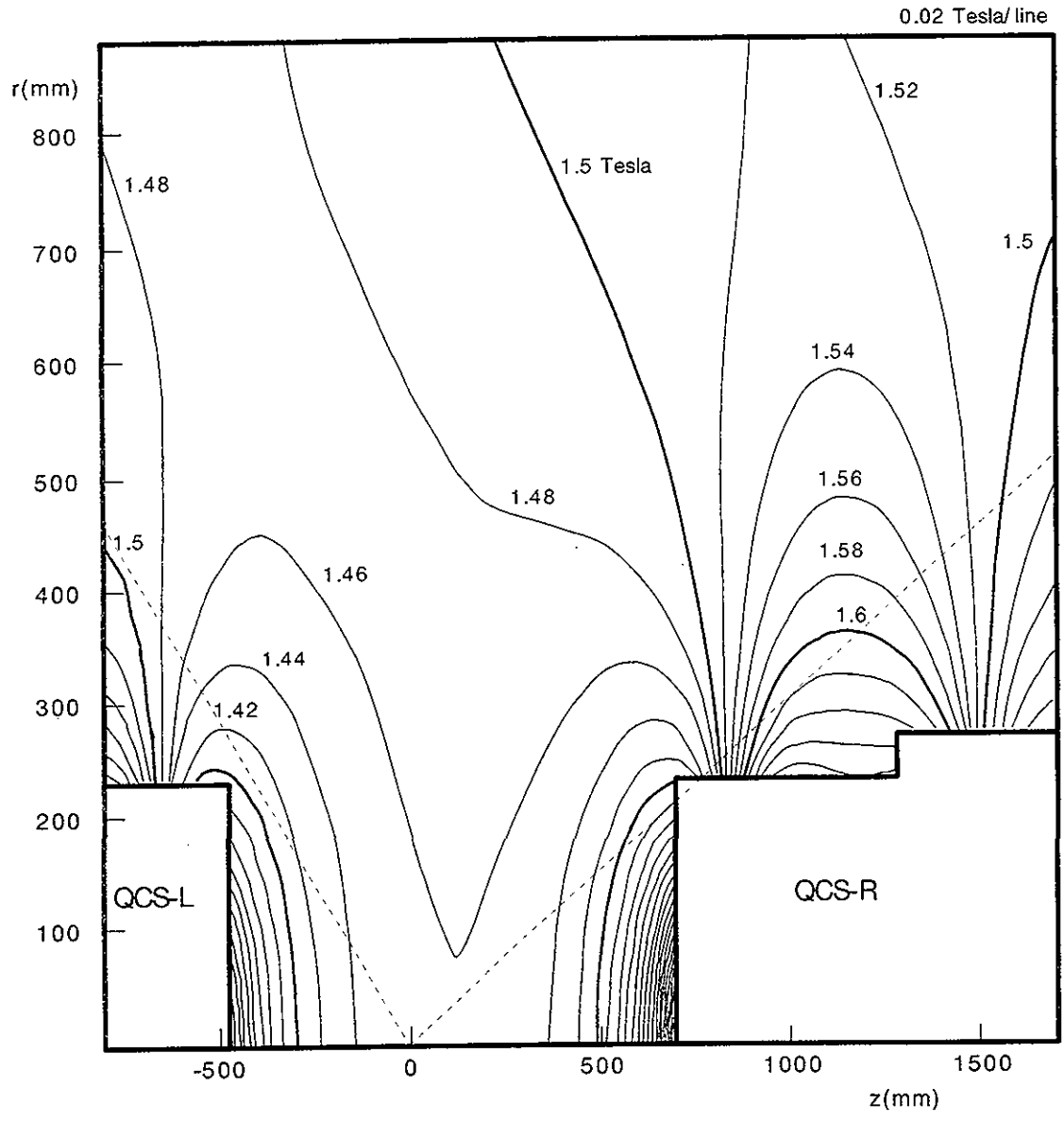

Fig. 7. A contour plot of the measured field in the Belle coordinate system with origin at the IP.

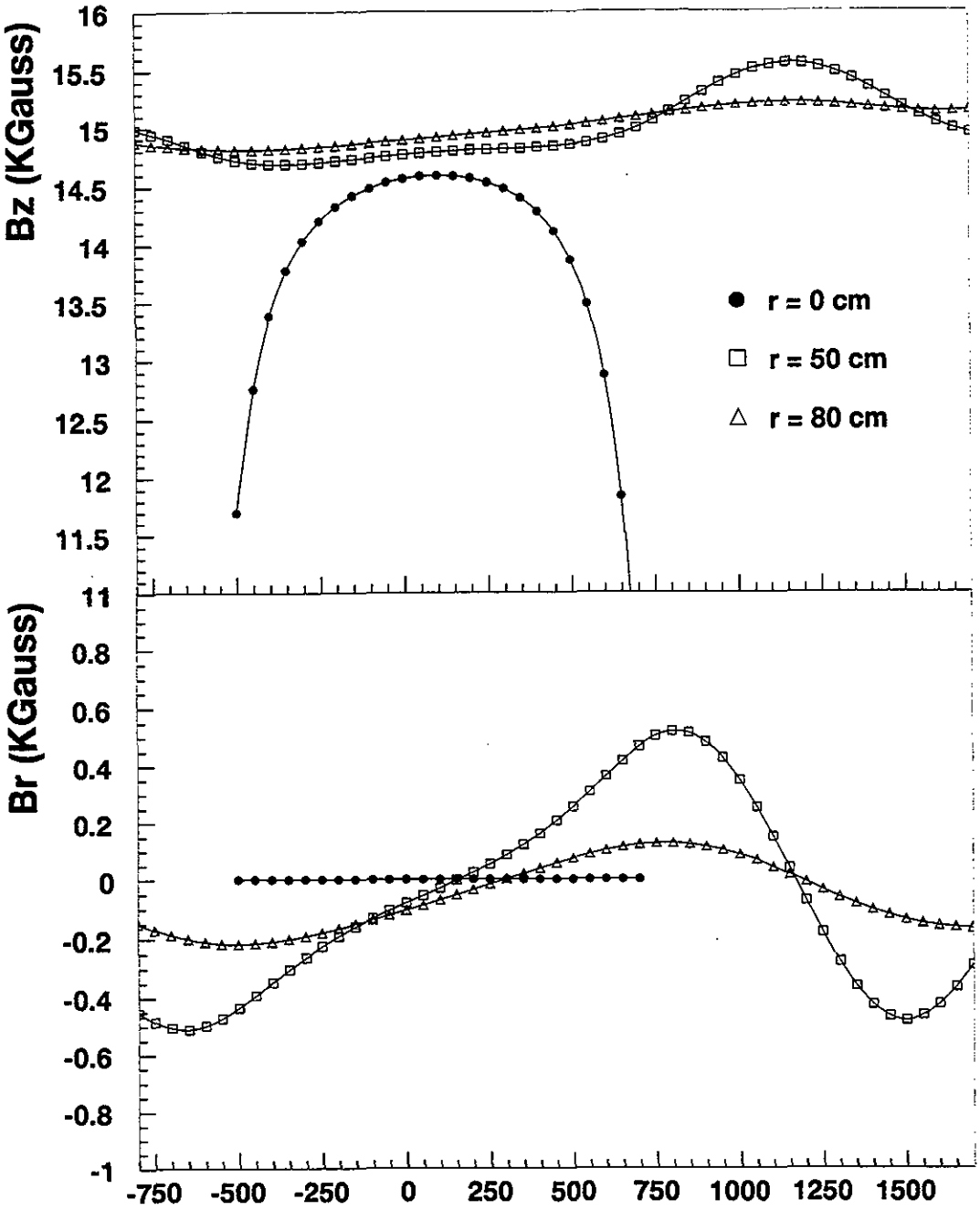

Fig. 8. The field strength as a function of z for different radii.

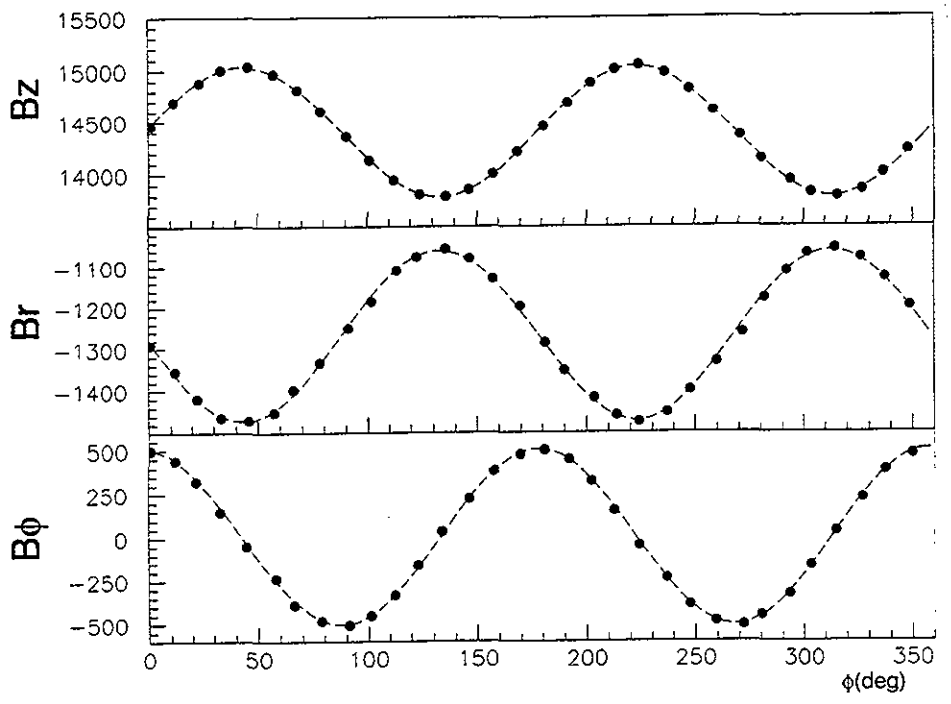

Fig. 9. The field distortions due to the quadrupole coil at r=300 and z=1600mm.

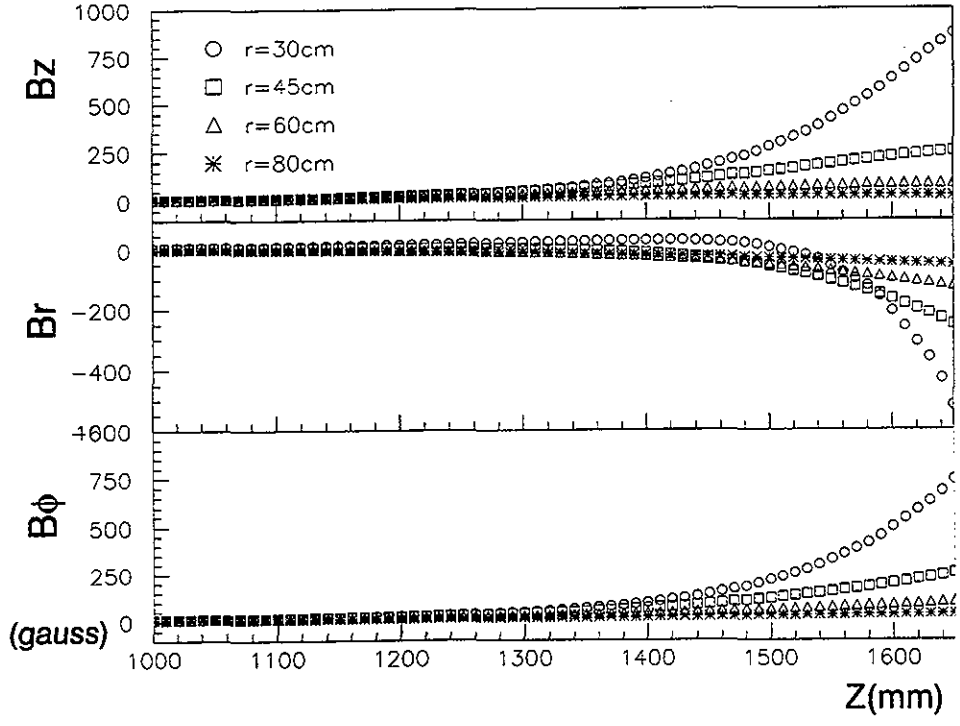

Fig. 10. The fitted values for the amplitude of the quadrupole field for each component for several radii as a function of z.

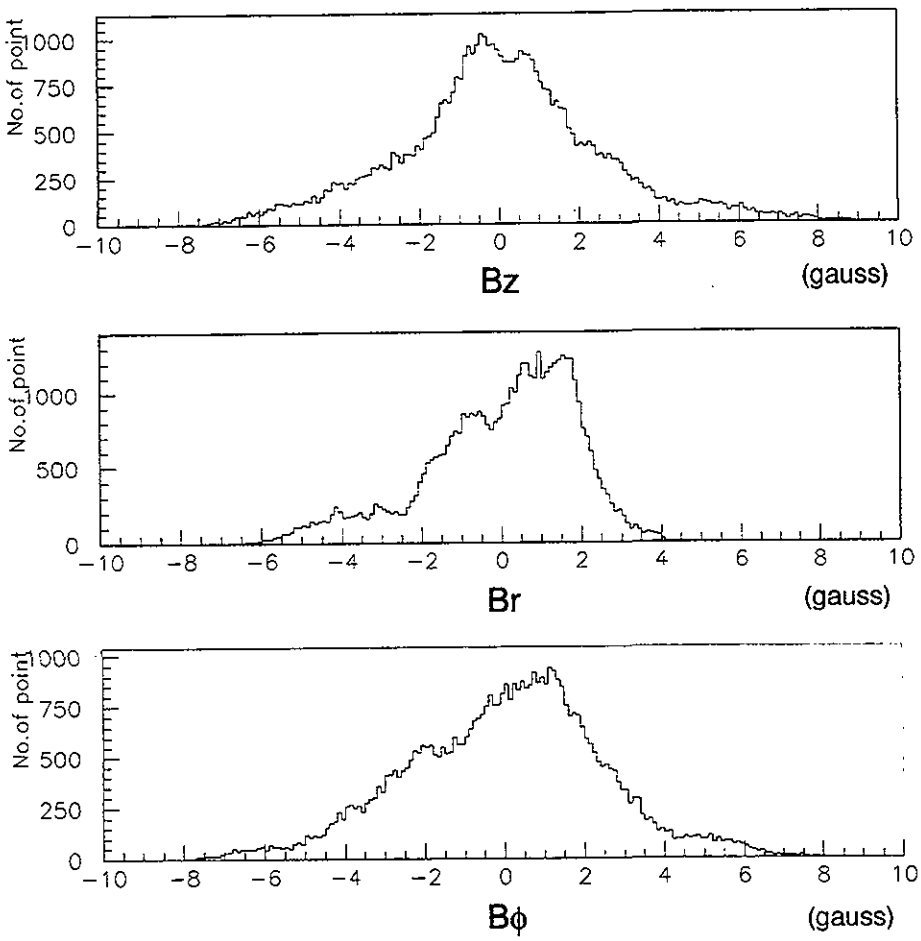

Fig. 11. The deviations of measured field components from their average over ϕ.

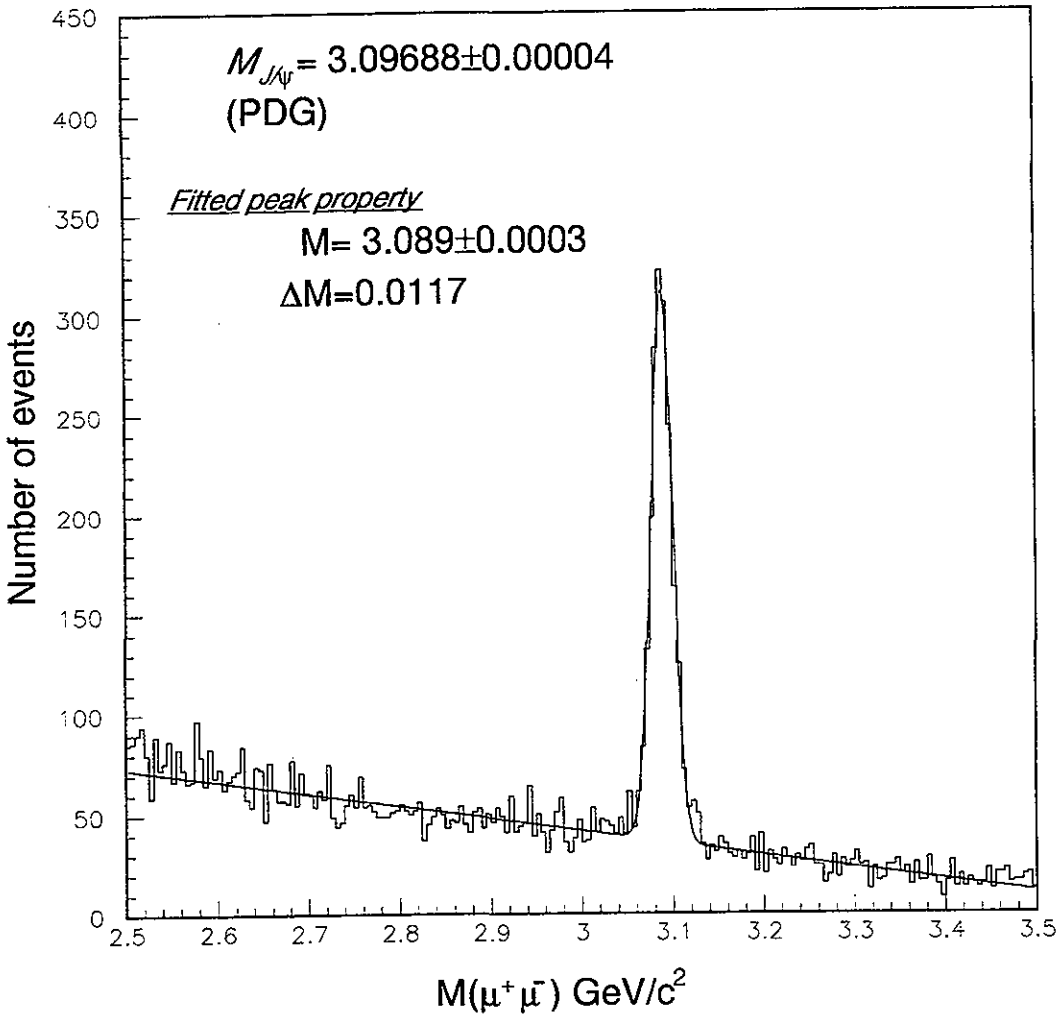

Fig. 12. Mass plot of J/ψ particles reconstructed in the Belle detector.